

In Vitro Assessment of Dialysis Membrane as an Endotoxin Transfer Barrier: Geometry, Morphology, and Permeability

*Michael Henrie, *Cheryl Ford, *Marion Andersen, *Eric Stroup, †Jose Diaz-Buxo, ‡Ben Madsen, ‡David Britt, and *Chih-Hu Ho

**Dialyzer R&D Department, Fresenius Medical Care North America, Ogden, UT; †Home Therapies Development, Fresenius Medical Care North America, Charlotte, NC; and ‡Biological Engineering Department, Utah State University, Logan, UT, USA*

Abstract: High-flux dialysis membranes used with bicarbonate dialysis fluid increase the risk of back diffusion of bacterial endotoxin into the blood during hemodialysis. Endotoxin transfer of various synthetic fiber membranes was tested with bacterial culture filtrates using an in vitro system testing both diffusive and convective conditions. Membranes were tested in a simulated dialysis mode with endotoxin challenge material (~420 EU/mL) added to the dialysis fluid, with saline used to model both blood and dialysis fluid. Samples were taken of both blood and dialysis fluid, and analyzed using a kinetic turbidimetric Limulus amoebocyte lysate assay. Endotoxin was found in all of the blood circuit samples, except for the Fresenius Optiflux F200NR[®] and thick-wall membranes. All membranes tested removed ~95% of the endotoxin from solution, with the residual ~5% recirculating within the dialysis fluid

compartment. Endotoxin distribution through the fiber membrane was examined using a fluorescent-labeled endotoxin conjugate. Fluorescence images indicate that adsorption occurs throughout the membrane wall, with the greatest concentration of endotoxin located at the inner lumen. Contact angle analysis was able to show that all membranes exhibit a more hydrophilic lumen and a more hydrophobic outer surface except for the polyethersulfone membranes, which were of equal hydrophobicity. Resulting data indicate that fiber geometry plays an important role in the ability of the membrane to inhibit endotoxin transfer, and that both adsorption and filtration are methods by which endotoxin is retained and removed from the dialysis fluid circuit. **Key Words:** Endotoxin—Hemodialysis membranes—Geometry—Dialysis fluid—Inflammation—Back filtration.

Recent advances in the management of end-stage renal disease using hemodialysis therapy have led to an increase in the widespread use of high-flux membranes and bicarbonate dialysis fluid (1–3). Scientific and clinical data support the use of high-flux membranes, as these have been shown to remove a larger portion of middle molecular weight toxins, particularly β_2 -microglobulin (4). Bicarbonate dialysis fluid is typically used in conjunction with high-flux membranes due to its biocompatibility (3).

Research has shown the use of bicarbonate dialysis fluid coupled with high-flux membranes to be associ-

ated with an increase in the chance for reactions stemming from cytokine-inducing substances (CIS) transferring across the dialysis membrane by way of back filtration (5–8). Contaminated water enters the dialysis machine and is mixed with bicarbonate concentrate, providing ideal environmental conditions for bacteria to proliferate (8,9). Pyrogenic reactions during hemodialysis may occur when dialysis fluid contaminants enter the blood compartment (BC) and subsequently the patient, which may lead to inflammation (5,10,11). Some dialysis patients experience chronic microinflammation, a periodical activation of blood cells by hemodialysis that may lead to the development of long-term dialysis-related conditions, including sepsis (1,12–15). A typical patient on hemodialysis therapy will be exposed to 18 000–30 000 L of water annually in the form of dialysis fluid (16,17), which may afford opportunities for blood contact with pyrogenic contaminants.

doi:10.1111/j.1525-1594.2008.00592.x

Received May 2007; revised October 2007.

Address correspondence and reprint requests to Dr. Chih-Hu Ho, Dialyzer R&D Department, Fresenius Medical Care North America, 475 West 13th Street, Ogden, UT 84404, USA. E-mail: chih-hu.ho@fmc-na.com

Endotoxin or lipopolysaccharide (LPS), a pyrogen of interest, is a surface-recognition constituent of Gram-negative bacterial membranes that is the most important CIS in contaminated dialysis fluid (18). Endotoxin is comprised of a heteropolysaccharide chain, a core oligosaccharide, and a bioactive lipid component termed lipid A, which determines its pyrogenicity (6,19). Endotoxin is an amphiphilic molecule, and will readily bind to hydrophobic surfaces and cationic material due to its hydrophobicity (10). The size of endotoxins varies from monomers of 10 kDa to micelles of 1000 kDa or larger (19–22). Thus, endotoxin is a complex molecule with many defining characteristics.

The majority of endotoxins found in dialysis fluid and water for dialysis fluid come from *Pseudomonas* contamination (16,23,24). Such bacteria are commonly found in most water supplies even after standard water treatment (8). However, clinical water systems may also be found to harbor bacterial biofilms due to improper design or neglect in microbiological monitoring, which are difficult to detect and remove (9,11,17). Numerous studies on water quality of dialysis clinics have been conducted in both the USA and Europe, with some reporting as many as 20% of the samples tested being above the limit of the recommended standards (4,18,22,24). There exist numerous investigations to remove endotoxin from circulating blood, including polymyxin B immobilization, charcoal hemoperfusion, and plasma exchange; however, few studies focus on endotoxin removal from dialysis fluid by the dialyzer (4,13,25).

To the hemodialysis patients, the membrane is the final barrier in preventing pyrogenic substances, such as endotoxins, from entering their blood during treatment and causing pyrogenic reactions (16). As the final barrier, the membrane needs to function as a trap for endotoxins, removing them from dialysis fluid, and preventing them from crossing into the BC (8,17). Prior experiments have shown significant differences in endotoxin permeability between similar dialysis membranes, suggesting that specific membrane characteristics contribute to the overall performance of inhibiting *trans*-membrane flux of endotoxins (26).

The objective of the present study was to investigate the removal mechanism of endotoxins for several different membranes, utilizing endotoxins from cultured sources as well as fluorescent-labeled conjugates. Membranes were tested *in vitro* using both convective and diffusive experimental setups to determine if the primary mechanism of pyrogen retention is adsorption, filtration, or a combination of the two working synergistically (13).

The working hypothesis for this study is that adsorption is the governing factor of endotoxin removal, with filtration also occurring. Furthermore, we investigated how the geometry of the dialysis fiber membrane, specifically the morphology and tortuosity of the fiber wall, would affect the ability of the membrane to prevent endotoxins transferring from the dialysate compartment to the patient bloodstream, highlighting those geometrical membrane features that enhance the performance of the membrane in endotoxin removal.

MATERIALS AND METHODS

Membranes

Both commercially available and laboratory-produced experimental membranes were used for this study. Fresenius Optiflux F200NR[®] membranes were used as the control group. The remaining membranes tested were laboratory-produced experimental membranes manufactured to represent the following membrane categories, so as to accentuate specific geometric characteristics: high flux, low flux, thick wall, thin wall, and macrovoid. (Macrovoids are large, open cavities found within the substructure of a polymeric membrane, formed during the phase inversion process.) These membranes were produced so that specific geometric qualities inherent within each membrane type could be evaluated against the control and the other groups, to distinguish which membrane characteristics exhibit the greatest influence on the ability of the membrane to adsorb endotoxin and inhibit endotoxin transfer. Dialysis membrane characteristics of interest include wall thickness, solute flux, inner and/or outer skin, macrovoids, hydrophobicity, and pore size distribution.

All fiber membranes used in this investigation were polysulfone (PS) except for the experimental macrovoid membrane, which was composed of polyethersulfone (PES). All experimental fibers were produced using the phase inversion solution precipitation method (27). Table 1 lists the characteristics of all the dialysis fiber membranes used in the study.

In vitro dialysis circuit

A model of *in vitro* dialysis previously described (17) was modified for this study (Fig. 1). Pumps connected to the BC and dialysis fluid compartment (DC) were first calibrated using sterile saline. Standard dialysis tubing sets (Medisystems, Elizabeth, CO, USA) were modified and sterilized prior to running the dialysis simulation, according to the experimental setup (Fig. 1). Both the BC and DC were then rinsed with pyrogen-free saline for no less

TABLE 1. Fiber characteristics for all dialysis membranes used in study

Fiber membrane	Fiber inner diameter (μm)	Fiber wall thickness (μm)	Sodium clearance (mL/min)	Albumin sieving (%)	Aqueous KUF (mL/h-mm Hg)
Optiflux F200NR ^c	185	35	277	0.45	200
Low flux	181	39	275	0.90	48
High flux	182	37	283	6.69	522
Thin wall	187	24	282	0.27	231
Thick wall	184	44	271	0.21	190
Macrovoid (PES)	212	33	271	2.53	130

than 15 min (4 L), to remove any residual endotoxins. Following the saline rinse, the simulation commenced by closing the BC circuit (closed loop) and introducing the dialysis fluid challenge solution (420 ± 24 EU/mL) to the DC circuit.

The flow through the BC circuit was held constant at 200 mL/min, while flow through the DC circuit was 500 mL/min. After 60 min, the experimental assembly was modified to run the convective setup; flow from the BC compartment was adjusted to 37 mL/min and the simulation was run for an additional 60 min after which the experiment was complete (17).

Samples of 10 mL were collected from both the BC and DC circuits following the saline rinse, and at time 0, 7, 15, 60, 67, 75, and 120 min. All samples were kept at 4–6°C until analyzed.

Dialysis fluid with bacterial culture filtrates

The contaminated dialysis fluid challenge solution was prepared by inoculating separate tryptic soy broth (TSB) media with *Senotrophomonas maltophilia* ATCC 13637 and *Pseudomonas aeruginosa* ATCC 27853. Following 48 h of incubation, cultures were ultrasonicated (2 min at room temperature) and successively filtered using decreasing pore size, with a resulting final filtration at 0.45 μm . The remaining

bacterial culture filtrates were then combined, rendering a challenge solution with LPS from both organisms.

Mixed culture filtrate and all test samples were analyzed for endotoxins using the kinetic turbidimetric Limulus amoebocyte lysate assay (Charles River Labs, Wilmington, MA, USA) to determine the concentration of endotoxins (EU/mL) in solution. The detection limit of the assay was 0.1 EU/mL. Culture filtrate analysis was conducted prior to inoculation of the dialysis fluid, so as to accurately add the desired amount of challenge EUs. The challenge dialysis fluid solution was kept at 4–6°C until used.

Fluorescent imaging

Fluorescent-labeled LPS conjugate was used to study the areas where endotoxin binding occurs throughout the membrane wall. Prior studies have shown that a fluorescent label attached to the LPS molecule does not affect the behavior of the endotoxins (28). Mini-modules (Fig. 2) were constructed for the fluorescent imaging portion of the study, to minimize the amount of fluorescent-labeled LPS conjugate required. Thirty fibers of each type were placed in a mini-housing (15 cm in length) and potted using UV-curable epoxy resin (Dymax Corp., Torrington, CT, USA). The mini-modules were

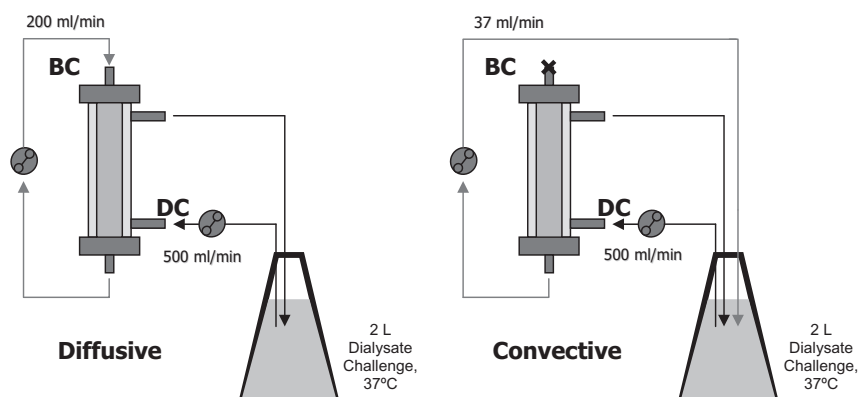


FIG. 1. Experimental dialysis simulation setup for the endotoxin challenge tests. The diffusive setup is first run for 60 min, after which the system is changed to the convective setup and run for an additional 60 min.

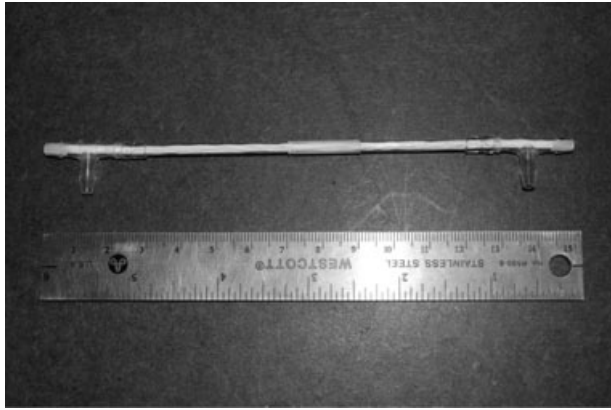


FIG. 2. Mini-module used for fluorescence imaging, showing polycarbonate housing and T's, with UV-curable epoxy for potting material. Approximately 30 fibers, 20 cm in length, provide the mini-module with about 20 cm² of surface area.

subjected to the same experimental simulation setup as the other membranes, with 60 min of diffusive and 60 min of convective testing. Alexa Fluor 594 conjugate (Invitrogen, Carlsbad, CA, USA) was used to contaminate the dialysis fluid. Each mini-module was subjected to a challenge of 30 mL of an 800 EU/mL solution of labeled LPS conjugate, with the simulation run in a controlled dark environment.

After the simulations were complete, mini-modules were placed in a drying oven to prepare for sectioning and imaging. The process of embedding, slicing, and imaging the samples used a previously described protocol modified for this study (29,30). Fiber membranes were removed from their housings and sectioned to 10 μ m using tissue-freezing media (Triangle Biomedical Sciences, Durham, NC, USA) and a cryostat (Leica 1850, Wetzlar, Germany). Sectioned fibers were imaged using fluorescent microscopy with a resorufin filter set (Chroma Technology, Rockingham, VT, USA). Images were obtained of the membrane samples using a 60 s image integration time.

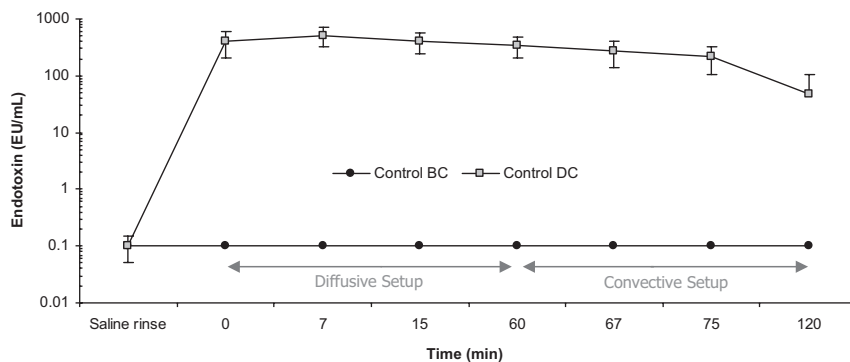


FIG. 3. Simulation data of the control (Optiflux F200NR[®]) membrane. The upper plot represents the DC, while the lower plot represents the BC. No BC samples contained endotoxins above the detection limit of 0.1 EU/mL for this particular membrane.

Surface characterization

For all membranes tested, sessile drop contact angle analysis was performed on both the outer surface and inner lumen of the fibers. To access the inner skin, the fiber was cut sagittally and spread open onto double-sided tape. A goniometer (AST Products, Billerica, MA, USA) was used to image a positioned 0.25 μ L droplet of distilled deionized water on the surface being tested. Immediately following the application of the droplet, a digital image was captured; from this image, the contact angle of the droplet was calculated.

Scanning electron microscopy (SEM) imaging

Fiber membranes were prepared for SEM imaging by dipping the fibers in liquid nitrogen and snapping them with a quick motion, resulting in a 90° break. The membrane samples were then fixed to an imaging stage and sputtered with gold (20 nm thick) using a sputter coater (Lesker 108, Clairton, PA, USA) and a thickness monitor (Cressington MTM10, Watford, U.K.), and imaged at 250 \times using an F4000 scanning electron microscope (Hitachi Ltd., Tokyo, Japan).

RESULTS

Dialyzer simulations using bacterial culture filtrates as challenge material

Dialysis simulation data for all membranes tested are presented in Figs. 3–6, with curves representing endotoxin levels measured from the BC and DC. The diffusive segment of the simulation occurred from minute 0 to minute 60, followed by the convective segment between minute 60 and minute 120. Typically, the maximum endotoxin concentration in the DC is represented by samples from minute 7 or minute 15. This is perhaps due to the time required for the endotoxin to equilibrate throughout the fluid volume contained in the DC. Each dialysis simulation plot shows that as the experiment progressed, the

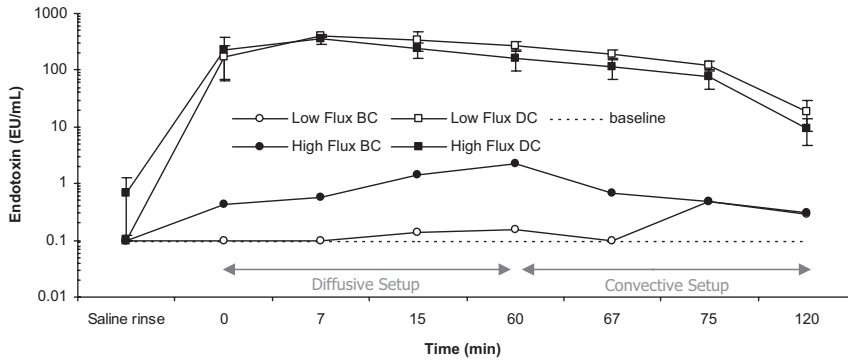


FIG. 4. Simulation data of high-flux and low-flux membranes. The detection limit has been represented by a baseline plot. The low-flux membrane exhibited better performance than the high-flux membrane, allowing less endotoxins to cross into the BC.

membrane removed free endotoxins from the DC, resulting in a steady decline in the DC endotoxin concentration.

The dialysis fluid reservoir endotoxin concentration measurements after bacterial culture filtrate addition and prior to simulation were as follows: control, 465 ± 40 EU/mL; high flux, 403 ± 53 EU/mL; low flux, 425 ± 53 EU/mL; thick wall, 428 ± 41 EU/mL; thin wall, 399 ± 102 EU/mL; PES macrovoid, 424 ± 89 EU/mL. Following the dialysis simulations, the data show that no endotoxin was detectable in any of the BC samples from both the control (Fig. 3) and the thick-wall (Fig. 5)

membranes, indicating that no detectable amounts of endotoxin were allowed to back diffuse into the BC.

For the remaining membranes, endotoxin concentrations in the BC were detectable following the initial endotoxin challenge and increased over time, with all of the membranes obtaining peak endotoxin concentrations in the BC during the convective portion of the experiments. Peak endotoxin concentrations measured for the remaining membrane types were as follows: high flux, 2.24 EU/mL at 60 min; low flux, 0.47 EU/mL at 75 min; thin wall, 2.47 EU/mL at 75 min; and PES macrovoid, 0.28 EU/mL at 60 min.

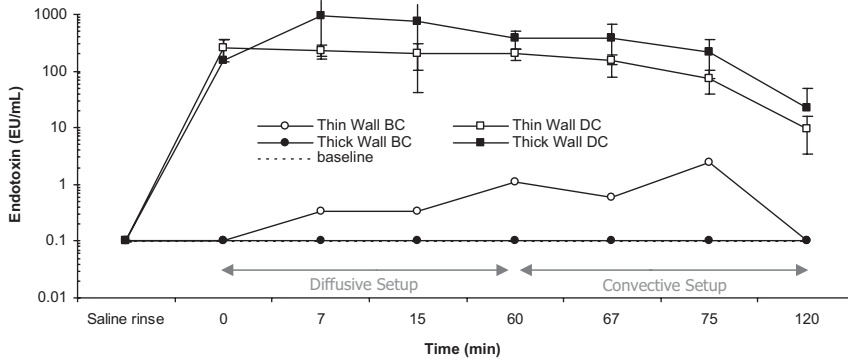


FIG. 5. Simulation data of thick-wall and thin-wall membranes. No BC samples from the thick-wall membrane contained detectable levels of endotoxins. At minute 120, the thin-wall membrane exhibited nearly nondetectable amounts of endotoxins in the BC after nearly 3 EU/mL from the previous sample.

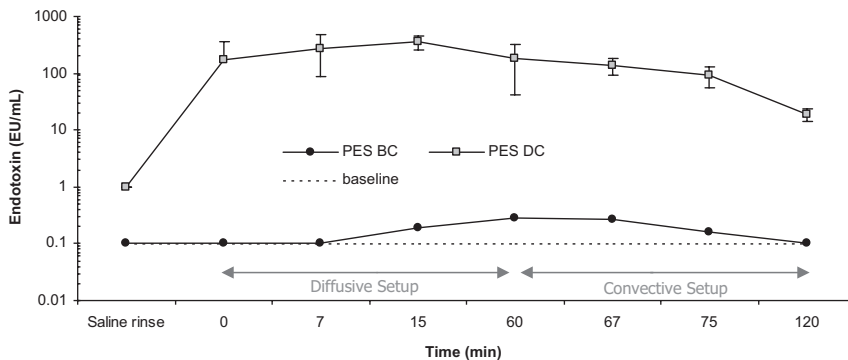


FIG. 6. Simulation data of the PES macrovoid membrane. Endotoxins in the BC start to increase in the diffusive portion, and are removed by the end of the experiment as the endotoxins in the DC are slowly removed from the system.

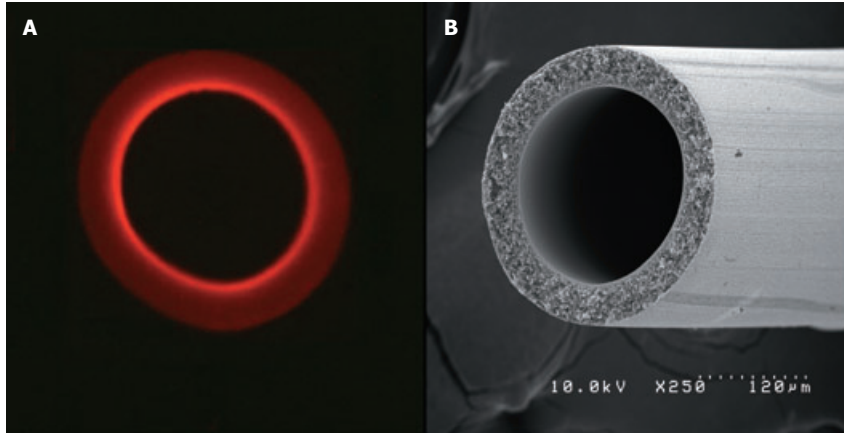


FIG. 7. Fluorescence image (A) and SEM image (B) for the Optiflux F200NR[®] fiber membrane (control). Fluorescent-labeled LPS conjugate is distributed throughout the entire membrane cross section, accumulating at the inner lumen surface.

Imaging of dialysis membranes

Fluorescence and SEM images for all membranes tested are presented in Figs. 7–12, with each fluorescence image showing the distribution of the fluorescently labeled endotoxin, and the SEM image showing the specific fiber membrane geometry including membrane substructure, and outer and

lumen skin surface characteristics. All fluorescence images show the endotoxin conjugate throughout the cross section of the fiber wall. The greatest fluorescent intensity for all membranes tested was located at the inner lumen of the fiber. All fluorescent images were taken at 1280 × 1024 resolution. No atypical fluorescent patterns were observed with any of the

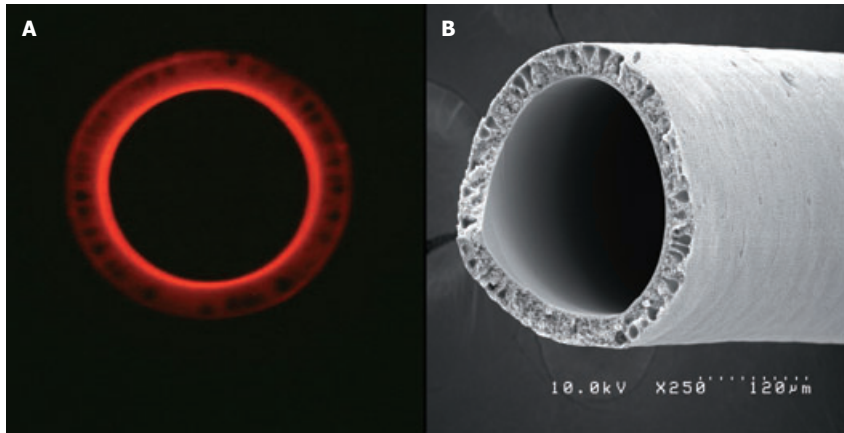


FIG. 8. Fluorescence image (A) and SEM image (B) for the PES macrovoid fiber membrane. Note how the macrovoids outlined in the fluorescence image are clearly defined in the SEM of the fiber end, and the width of the high-intensity fluorescence present at the lumen.

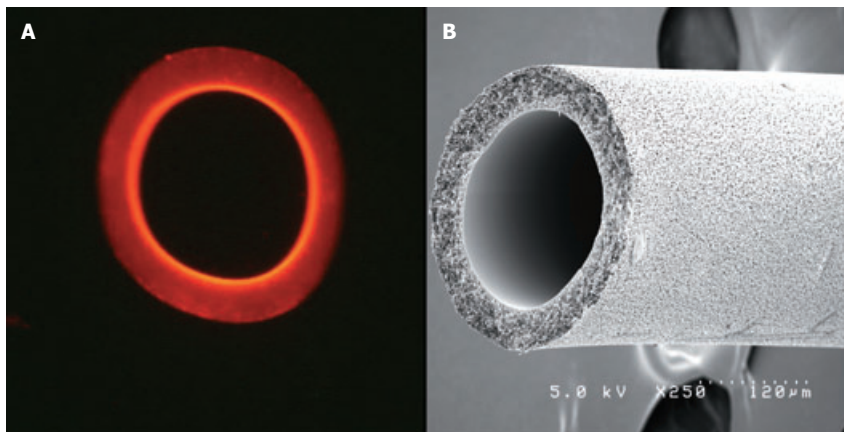


FIG. 9. Fluorescence image (A) and SEM image (B) for the high-flux fiber membrane. The intensity observed at the lumen is thin compared to other fiber types, indicating that more of the endotoxins are distributed throughout the fiber substructure, which can be supported by the heightened fluorescence intensity throughout the section. The SEM image reveals the increase in porosity of the outer surface of the membrane.

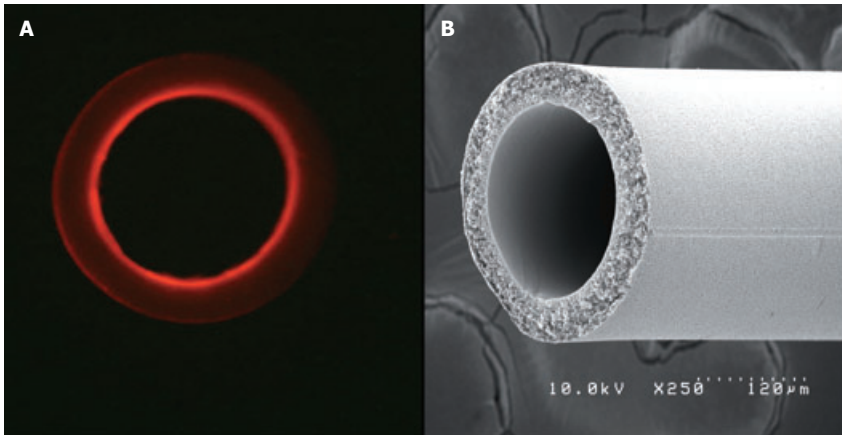


FIG. 10. Fluorescence image (A) and SEM image (B) for the low-flux fiber membrane. The porosity of the outer skin is much less than that of the high flux (Fig. 9), as seen in the SEM. The majority of the fluorescence found within the membrane cross section is located at the lumen surface.

membrane images; all cut sections exhibited similar fluorescence to these representative images.

Surface hydrophobicity by contact angle analysis

Contact angle measurements were performed on both the outer and inner skin of the fiber membrane. Results for the contact angle measurements are

depicted in Fig. 13, with mean \pm standard deviation ($n = 5$). Statistical analysis was conducted to show significant difference between outer and inner lumen contact angles. Results indicate that the thick-wall, thin-wall, high-flux, and Optiflux F200NR^e membranes exhibited significant differences between the outer and inner skin contact angles ($P < 0.05$).

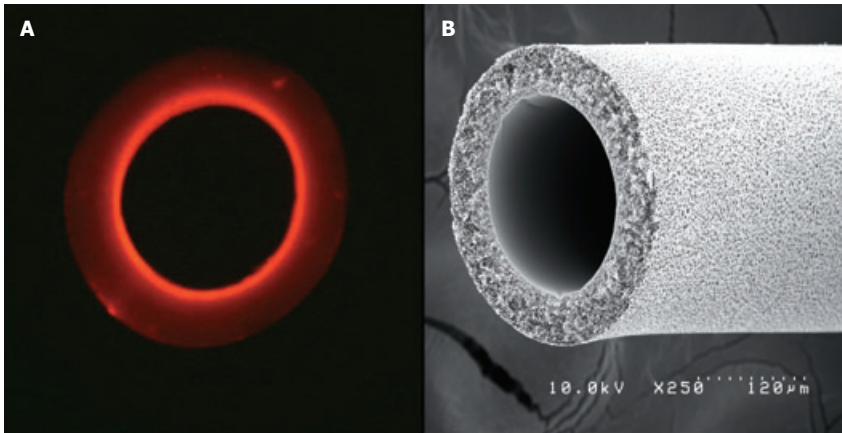


FIG. 11. Fluorescence image (A) and SEM image (B) for the thick-wall fiber membrane. The thick-wall membrane was only one of two membranes to block all detectable amounts of endotoxins from back filtrating, and this performance could be partially attributed to the larger surface area provided from the thick membrane.

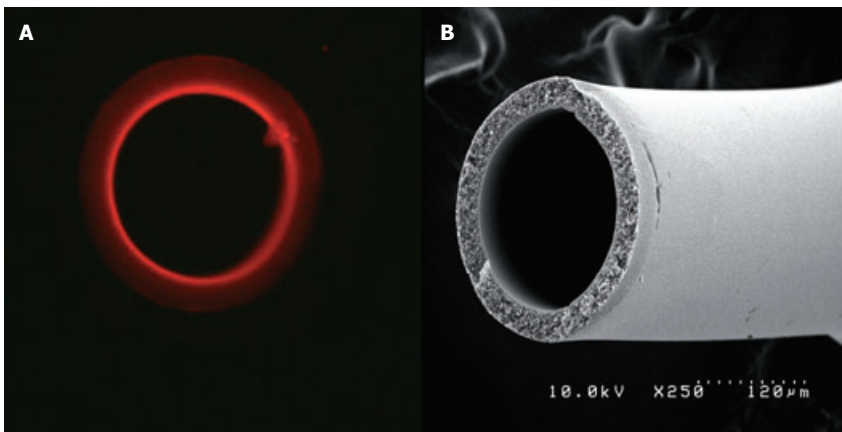


FIG. 12. Fluorescence image (A) and SEM image (B) for the thin-wall fiber membrane. The outer surface of the thin wall is much less open and porous than the outer surface of the thick-wall membrane (Fig. 10). The fluorescence image reveals that the majority of the endotoxins retained within the fiber substructure are concentrated at the lumen, in stark contrast to the remainder of the membrane section.

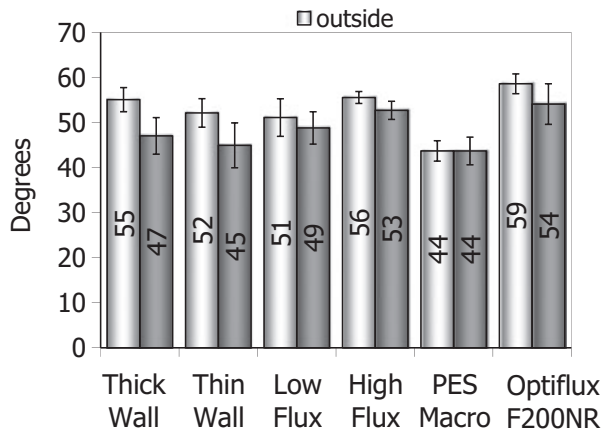


FIG. 13. Contact angle measurements of both inner lumen and outer skin of fiber membrane (mean \pm standard deviation, $n = 5$). A t -test revealed significant difference between the outside and lumen side contact angle for all membranes except low flux and PES macrovoid ($P < 0.05$).

From the graph, we observed that for all PS fiber membranes, the contact angle obtained from the inner lumen is less than that of the outer skin, indicating the lumen surface contains more hydrophilic domains or is a much smoother surface than the outer skin. The hydrophilic lumen could also be related to a localized amount of polyvinylpyrrolidone (PVP), a hydrophilic component used in the membrane production process, which may be congregating near the lumen surface.

Only the PES macro and low-flux membranes exhibited similar contact angles for both outer and inner surfaces of the membrane. Similar results could be indicative of smooth outer and inner membrane skins, or perhaps a more homogeneous distribution of PVP within the membrane structure.

DISCUSSION

The topic of endotoxins in nephrology typically revolves around the quality of dialysis water used for dialysate preparation, while this study focused on the capability of the membrane as an endotoxin adsorbent or filter, from a material science viewpoint.

As the frequency of use of high-flux dialysis coupled with bicarbonate dialysate increases, the need to discuss and analyze the role of the membrane as a barrier to the transfer of CIS also increases. Multiple studies have shown that CIS other than endotoxins are capable of eliciting a pyrogenic response (15,31); recent research has shown the body's response to endotoxins, specifically the kidney (12,32). Currently, there is a considerable amount of

research being conducted on the pyrogenicity of bacterial DNA and its impact on patients dealing with renal failure (33,34).

Further research into these smaller CIS and their role in contaminated dialysate is necessary in order to determine all possibilities in which a dialysis patient may experience inflammation due to bacterial infection, and how to design a membrane that counteracts this phenomenon (5). However, of all the CIS, the most important is endotoxin due to lipid A, and its elevated pyrogenicity and ability to induce blood cells (34,35). The aims of this study were to determine the geometry-specific attributes of a membrane that aid in its ability to retain endotoxins within the fiber wall, and to observe the distribution of retained endotoxins within the membrane.

The saline/saline model used for this study was effective for our purpose, to test the limits of the membrane exclusively with no external environmental factors requiring attention; effects of blood protein adsorption do not require consideration with data obtained from these simulations. Previous studies using blood in the BC have shown that endotoxins and other CIS, following back diffusion, may adsorb to proteins found coating the BC, thus altering the detectable *trans*-membrane flux (23,27,36). This protein layer typically forms on the blood side membrane surface during hemodialysis treatment and in vitro studies using blood. The experimental setups detailed within this study examined the membrane interaction with endotoxin in a controlled, sterile, and protein-free environment. Whole blood models are useful for endotoxin research, such as when testing for CIS back diffusion by monitoring monocyte activation (11,20,24). However, cytokine analysis was not included in this study as experiments focused on material and geometry-specific properties of the membranes.

The challenge material used for this study, bacterial culture filtrate, was chosen for its clinical relevance; *Pseudomonas* accounts for the majority of dialysis water contaminants (3,36). As bacterial culture filtrates are introduced into the DC, an array of bacterial products are present, many of which are capable of eliciting a pyrogenic response (9,21). However, this study focused on endotoxins specifically and how the amphiphilic nature of LPS affects its subsequent interaction with a dialysis membrane in an in vitro environment.

For these experiments, the endotoxin challenge concentration was roughly 20 times the allowable amount for medical devices. A relatively high concentration of challenge material was necessary to exploit all avenues of endotoxin removal, as well as

thoroughly testing the capacity of the membrane, considering the high rejection rate for the membranes (>99.99%) to detect endotoxins in the BC. Given the typical clinical situation where dialysis fluid levels of endotoxin concentration are routinely <5 EU/mL for 90% of all tested samples (36), the endotoxin concentrations used for the present study are significantly higher and could be considered a "worst case scenario." Consequently, the Association for the Advancement of Medical Instrumentation and European Pharmacopoeia limits for endotoxins in dialysis water are 2 and 0.25 EU/mL, respectively.

Results from the high-flux and low-flux simulations suggest that the KUF of the dialysis membrane will affect the extent of fluid back transport and subsequent flux of pyrogenic material. Data show the low-flux membrane was better than the high-flux at inhibiting endotoxins from accessing the BC during the experiment, implying that a smaller lumen pore size distribution may help in membrane performance. This supports the theory that a highly permeable membrane with a larger pore size distribution will increase the opportunity for pyrogen-containing dialysis fluid to back diffuse (17,37).

From the collected data, we conclude that membrane geometry plays a vital role in the inhibition of endotoxin transfer. Differences in thick-wall and thin-wall simulation data suggest that fiber tortuosity, the "path" that endotoxin would follow from the DC to the BC, affects the endotoxin *trans*-membrane flux by determining diffusive resistance (18,36). Thin-wall data show endotoxins in the BC after 7 min, increasing in concentration throughout the experiment until the final minutes, when most of the endotoxins have been removed from the dialysate circuit. This supports the theory that a longer "path," such as that exhibited by the thick-wall membrane, provides more available membrane surface area for endotoxin adsorption to occur (18).

The importance of membrane tortuosity is also supported by the observed results for the PES membrane, where endotoxins were able to cross into the BC from as early as the minute 15 sample. The PES fiber was the only membrane structure to exhibit macrovoids. These macrovoids imply a situation where the tortuosity of the membrane is compromised, as endotoxins would more easily pass from the outer wall to the inner lumen of the fiber when compared to a fiber composed of an asymmetrical sponge structure. Therefore, tortuosity imparts a significant contribution to membrane performance.

Surface energy of the membrane determines where adsorptive removal of endotoxins will occur. Fluorescence imaging shows that endotoxin adsorp-

tion is occurring practically everywhere throughout the fiber membranes. Contact angle analysis shows the overall trend from a hydrophobic outer surface to a more hydrophilic lumen surface for all the PS membranes. The results agree with earlier studies showing the relatively high capacity of PS and PES fiber membranes for endotoxin adsorption (22,23,36). When macrovoids are present within the fiber section, they decrease the total amount of surface area within the fiber wall, thus limiting the opportunity for endotoxins to adsorb to a hydrophobic surface (35).

During the simulations, as dialysis fluid was recirculated through the DC, the amount of free endotoxins in the solution decreases as the fiber membrane effectively adsorbs and filters the endotoxins out of the solution, thus removing them from circulation (38). The average reduction in endotoxins in the DC for all membranes tested was 95.4%, showing that over the course of the 2 h experiment, nearly 96% of the initial challenge endotoxins are removed from the solution.

One interesting observation regarding adsorption is that with all membranes tested, the endotoxin concentration of the 120 min DC sample, when compared with the prior samples, exhibits a negative slope. This outcome reinforces the assumption that the adsorptive capacity of the membrane had not yet been saturated with the amount of endotoxins used for this study (~420 EU/mL). This finding agrees with a previous study that reported high levels (380 pg/mL) of LPS in dialysis fluid do not necessarily lead to pyrogenic reactions (3), possibly due to the retention properties of the dialysis membrane.

CONCLUSION

As the use of high-flux dialysis membranes coupled with bicarbonate dialysis fluid increases, the necessity to guard against possible pyrogen- and CIS-induced inflammatory reactions is reaffirmed. Not only should efforts be made to generate ultrapure dialysate, but also to conduct thorough testing of all membranes currently in use for their ability to protect against bacterial contamination, and their individual ability to inhibit endotoxin transfer.

The ability of a dialysis membrane to retain endotoxin within the fiber wall, as well as inhibit the transfer of endotoxin across the fiber membrane, is a complex process—a combination of material characteristics, environmental conditions, and contaminant concentration. Experimental results were unable to illustrate which membrane characteristic is the most influential relating to endotoxin inhibition, neither

accepting nor rejecting our hypothesis. However, after scrutinizing all the collected data from each experiment, it was determined that the overall performance of a membrane regarding inhibition of endotoxin *trans*-membrane flux is governed by a collective function of adsorptive capacity, membrane thickness (tortuosity), and lumen pore size distributions.

REFERENCES

1. Canaud B, Bosc J, Leray H, Morena M, Stec F. Microbiologic purity of dialysate: rationale and technical aspects. *Blood Purif* 2000;18:200–13.
2. Oliver J, Bland L, Oettinger C, et al. Bacteria and endotoxin removal from bicarbonate dialysis fluids for use in conventional, high-efficiency, and high-flux hemodialysis. *Artif Organs* 1992;16:141–5.
3. Gordon S, Oettinger C, Bland L, et al. Pyrogenic reactions in patients receiving conventional, high-efficiency, or high-flux hemodialysis treatments with bicarbonate dialysate containing high concentrations of bacteria and endotoxin. *J Am Soc Nephrol* 1992;2:1436–44.
4. Linnenweber S, Lonnemann G. Pyrogen retention by the Asahi APS-650 polysulfone dialyzer during in vitro dialysis with whole human donor blood. *ASAIO J* 2000;46:444–7.
5. Teehan G, Guo D, Perianayagam M, Balakrishnan V, Pereira B, Jaber B. Reprocessed (high-flux) Polyflux dialyzers resist *trans*-membrane endotoxin passage and attenuate inflammatory markers. *Blood Purif* 2004;22:329–37.
6. Bland L, Oliver J, Arduino M, Oettinger C, McAllister S, Favero M. Potency of endotoxin from bicarbonate dialysate compared with endotoxins from *Escherichia coli* and *Shigella flexneri*. *J Am Soc Nephrol* 1994;5:1634–7.
7. Nakatani T, Tsuchida K, Sugimura K, Yoshimura R, Takemoto Y. Response of peripheral blood mononuclear cells in hemodialyzed patients against endotoxin and muramyl dipeptide. *Int J Mol Med* 2002;10:469–72.
8. Roth V, Jarvis W. Outbreaks of infection and/or pyrogenic reactions in dialysis patients. *Semin Dial* 2000;13:92–6.
9. Hoenich N, Levin R. The implications of water quality in hemodialysis. *Semin Dial* 2003;16:492–7.
10. Rietschel E, Kirikae T, Schade F, et al. Bacterial endotoxin: molecular relationships of structure to activity and function. *FASEB J* 1994;8:217–25.
11. Marion-Ferey K, Leid J, Bouvier G, Pasmore M, Husson G, Vilagines R. Endotoxin level measurement in hemodialysis biofilms using “the whole blood assay.” *Artif Organs* 2005;29:475–81.
12. Nath K. Renal response to repeated exposure to endotoxin: implications for acute kidney injury. *Kidney Int* 2007;71:477–9.
13. Tetta C, Bellomo R, Inguaggiato P, Wratten M, Ronco C. Endotoxin and cytokine removal in sepsis. *Ther Apher* 2002;6:109–15.
14. Hsu P, Lin C, Yu C, et al. Ultrapure dialysate improves iron utilization and erythropoietin response in chronic hemodialysis patients—a prospective cross-over study. *J Nephrol* 2004;17:693–700.
15. van Tellingen A, Grooteman M, Pronk R, et al. Lipopolysaccharide concentrations during superflux dialysis using unfiltered bicarbonate dialysate. *ASAIO J* 2002;48:383–8.
16. ANZSN. *Consensus Statement for Maintenance of Chemical and Microbiological Safety of Haemodialysis Water and Dialysate Systems*. Sydney, Australia: Australian and New Zealand Society of Nephrology, 1996.
17. Weber V, Linsberger I, Rossmann E, Weber C, Falkenhagen D. Pyrogen transfer across high- and low-flux hemodialysis membranes. *Artif Organs* 2004;28:210–7.
18. Lonnemann G. Chronic inflammation in hemodialysis: the role of contaminated dialysate. *Blood Purif* 2000;18:214–23.
19. Gorbet M, Sefton M. Endotoxin: the uninvited guest. *Biomaterials* 2005;26:6811–7.
20. Yamamoto K, Matsuda M, Hayama M, et al. Evaluation of the activity of endotoxin trapped by a hollow-fiber dialysis membrane. *J Memb Sci* 2006;272:211–6.
21. Memoli B. Cytokine production in haemodialysis. *Blood Purif* 1999;17:149–58.
22. Czermak P, Ebrahimi M, Catapano G. New generation ceramic membranes have the potential of removing endotoxins from dialysis water and dialysate. *Int J Artif Organs* 2005;28:694–700.
23. Tsuchida K, Nakatani T, Sugimura K, Yoshimura R, Matsuyama M, Takemoto Y. Biological reactions resulting from endotoxin adsorbed on dialysis membrane: an in vitro study. *Artif Organs* 2004;28:231–4.
24. Jaber B, Gonski J, Cendoroglo M, et al. New polyether sulfone dialyzers attenuate passage of cytokine-inducing substances from *Pseudomonas aeruginosa* contaminated dialysate. *Blood Purif* 1998;16:210–9.
25. Sato T, Shoji H, Koga N. Endotoxin adsorption by polymyxin B immobilized fiber column in patients with systemic inflammatory response syndrome: the Japanese experience. *Ther Apher Dial* 2003;7:252–8.
26. Bommer J, Becker K, Urbaschek R. Potential transfer of endotoxin across high-flux polysulfone membranes. *J Am Soc Nephrol* 1996;7:883–8.
27. Mulder M. *Basic Principles of Membrane Technology*. Dordrecht, The Netherlands: Kluwer Academic Publishers, 1996.
28. Levels J, Abraham P, van den Ende A, van Deventer S. Distribution and kinetics of lipoprotein-bound endotoxin. *Infect Immun* 2001;69:2821–8.
29. Hayama M, Miyasaka T, Mochizuki S, et al. Optimum dialysis membrane for endotoxin blocking. *J Memb Sci* 2003;219:15–25.
30. Hayama M, Miyasaka T, Mochizuki S, et al. Visualization of distribution of endotoxin trapped in an endotoxin-blocking filtration membrane. *J Memb Sci* 2002;210:45–53.
31. Schindler R. Inflammation and dialysate quality. *Hemodial Int* 2006;10:S56–9.
32. Zager R, Johnson A, Lund S. Endotoxin tolerance: TNF- α hyper-reactivity and tubular cytoresistance in a renal cholesterol loading state. *Kidney Int* 2007;71:496–503.
33. Ratanarat R, Cazzavillan S, Ricci Z, et al. Usefulness of a molecular strategy for the detection of bacterial DNA in patients with severe sepsis undergoing continuous renal replacement therapy. *Blood Purif* 2007;25:106–11.
34. Schindler R, Beck W, Deppisch R, et al. Short bacterial DNA fragments: detection in dialysate and induction of cytokines. *J Am Soc Nephrol* 2004;15:3207–14.
35. Chanard J, Lavaud S, Randoux C, Rieu P. New insights in dialysis membrane biocompatibility: relevance of adsorption properties and heparin binding. *Nephrol Dial Transplant* 2003;18:252–7.
36. Lonnemann G, Sereni L, Lemke H, Tetta C. Pyrogen retention by highly permeable synthetic membranes during in vitro dialysis. *Artif Organs* 2001;25:951–60.
37. Takemoto Y, Nakatani T, Sugimura K, Yoshimura R, Tsuchida K. Endotoxin adsorption of various dialysis membranes: in vitro study. *Artif Organs* 2003;27:1134–42.
38. Nakatani T, Tsuchida K, Sugimura K, Yoshimura R, Takemoto Y. Investigation of endotoxin adsorption with polyether polymer alloy dialysis membranes. *Int J Mol Med* 2003;11:195–7.